Northumbria Research Link

Northumbria University
NEWCASTLE

University**Library**

Evaluating the Impact of Multi-Carrier Energy Storage Systems in Optimal Operation of Integrated Electricity, Gas and District Heating Networks

Mohammad Amin Mirzaei[1,*], Morteza Nazari Heris[1], Kazem Zare[1], Behnam Mohammadi-Ivatloo[1], Mousa Marzband[2,3], Somayeh Asadi[4], Amjad Anvari-Moghaddam[5]

[1]Faculty of Electrical and Computer Engineering, University of Tabriz, Tabriz, Iran

[2]Department of Mathematics, Physics and Electrical Engineering, Northumbria University, Newcastle, England

[3]Center of Research Excellence in Renewable Energy and Power Systems, King Abdulaziz University, Jeddah, Saudi Arabia

[4]Dept. of Architectural Engineering, Pennsylvania State Univ., 104 Engineering Unit A, University Park, PA 16802.2

[5]Department of Energy Technology, Aalborg University, 9220 Aalborg, Denmark

[*]Corresponding author: Mohammad Amin Mirzaei

Abstract

Various energy networks such as electricity, natural gas, and district heating can be connected by emerging technologies for efficient application of renewable energy sources. On the other hand, the pressure shortage in the natural gas network and increasing heat loss in the district heating network by growth of gas and heat load in winter might play a significant role in the participation of combined heat and power units in the energy markets and operation cost of the whole integrated energy system. Hence, this paper presents a multi-network constrained unit commitment problem in the presence of multi-carrier energy storage technologies aiming to minimize the operation cost of an integrated electricity, gas and district heating system while satisfying the constraints of all three networks. In addition, an information gap decision theory is developed for studying the uncertainty of energy sources under risk-seeker and risk-averse strategies with no need for probability distribution function. Moreover, the role of multi-carrier energy storage technologies in integrated networks is investigated,

which indicates decrement of total operation cost and reduction of the effect of wind power uncertainty on total operation cost in presence of the storage technologies.

Keywords: Multi-network constrained unit commitment; District heating network; Gas network, Multi-carrier energy storage; Information gas decision theory; Wind energy**.**

Nomenclature

Indices and sets

t	Time interval
g	Gas supplier
i	Generation unit
wf	Wind turbine
b, b'	Power system bus
m, n	Gas network node
h	Heat system node
j	Electrical load
gl	Gas load
hl	Heat load
L	Power system transmission line
gs	Gas storage unit
hs	Heat storage unit
e	Power storage unit
pl	Gas pipeline
hp	Heat pipeline
NT	Total scheduling time horizon

NJ	Total electrical load
NGL	Total gas load
NHL	Total heat load
NE	Total non-gas-fired units
NG	Total gas-fired units
NC	Total CHP units
NGC	Total CHP and gas-fired units
NES	Total power storage units
NGS	Total gas storage units
NHS	Total heat storage units
NU	Total number of generation units
NWF	Total number of wind turbines
NHP	Total number of heat network pipelines
NPL	Total number of gas network pipelines
NB	Total number of power network buses

Input Parameters

$a_i, b_i, c_i, d_i, e_i, f_i$	Cost coefficients of the generation unit i
$P_i^{\max}, P_i^{\min}$	Minimum and maximum power supply of the generation unit i
$P_e^{D,\max}, P_e^{C,\max}$	Maximum charge/discharge capacity of the power storage unit e
$P_e^{D,\min}, P_e^{C,\min}$	Minimum charge/discharge capacity of the power storage unit e
$B_{hs}^{\text{Max, charge}}, B_{hs}^{\text{Max, discharge}}$	Maximum charge/discharge rate of the heat storage unit hs
$GS_{gs,\max}^{out}, GS_{gs,\max}^{in}$	Maximum produced/supplied gas of the gas storage unit gs
$A_e^{\max}, A_e^{\min}$	Minimum and maximum energy capacity of the power storage unit e

$B_{hs}^{\mathrm{Max}}, B_{hs}^{\mathrm{Min}}$	Maximum and minimum capacity of the heat storage *hs*
$E_{gs}^{\max}, E_{gs}^{\min}$	Maximum and minimum capacity of the gas storage *gs*
T_i^{On}, T_i^{Off}	Minimum on/off time interval of the generation unit *i*
$PF_L^{\max}$	Power transmission capacity of the line *L*
X_L	Reactance of the power system line *L*
$D_{j,t}$	Power system load *j* of at time *t*
$HL_{hl,t}$	Heat network load *hl* at time *t*
HR_e	Heat rate of the power storage unit *e*
$\eta_{hs}, \eta_{hs}^{ch}, \eta_{hs}^{dis}$	Standby/charge/discharge efficinecy
η_e^C, η_e^D	Charge/discharge efficiency of the power storage system *e*
$\eta_{gs}^{in}, \eta_{gs}^{out}$	Charge/discharge efficiency of the gas storage system *gs*
$T_h^{\max}, T_h^{\min}$	Minimum and maximum temperature at heat network node *h*
$\pi_m^{\max}, \pi_m^{\min}$	Maximum and minimum pressure at gas network node *m*
$GW_g^{\max}, GW_g^{\min}$	Minimum and maximum gas supply using gas petroleum *g*
$GL_l^{\max}, GL_l^{\min}$	Maximum and minimum gas load *l*
$HP_{hp}^{\max}, HP_{hp}^{\min}$	Maximum and minimum capacity of the heat pipeline *hp*
$P_{wf,t}$	Predicted wind power at time *t*
Le_{hp}	Length of the heat pipeline *hp*
$PF_L^{\max}$	Power capacity of the line *L*

Variables

$P_{i,t}$	Power generation of unit *i* at time *t*
$I_{i,t}$	On/off status of unit *i* at time *t*

$I_{e,t}^{C}, I_{e,t}^{D}$	Charge/discharge status of the power storage *e* at time *t*
$H_{i,t}$	Heat generated of CHP *i* at time *t*
$PF_{L,t}$	Power flow of the line *L* at time *t*
$X_{i,\,t-1}^{on}$, $X_{i,\,t-1}^{off}$	On/off time of unit *i*
$HP_{hp,t}$	Mass flow rate of heat pipeline at time *t*
$T_{h,t}$	Water temperature at node *h* at time *t*
$T_{h,t}^{back}$	Returning water temperature at node *h* at time *t*
$E_{gs,t}$	Available gas level in gas storage *gs* at time *t*
$B_{hs,t}$	Available heat energy level in heat storage *hs* at time *t*
$HD_{hs,t}^{dis}, HS_{hs,t}^{ch}$	Supplied/stored heat energy in heat storage *hs* at time *t*
$HDQ_{hs,t}, HCQ_{hs,t}$	Mass flow rate of heat storage in discharge and charge mode at time *t*
$HQ_{i,t}$	Mass flow rate of CHP at time *t*
$HLQ_{hl,t}$	Mass flow rate of heat load *hl* at time *t*
$P_{e,t}^{D}, P_{e,t}^{C}$	Discharge/charge power of the storage *e* at time *t*
$GS_{gs,t}^{out}, GS_{gs,t}^{in}$	Supplied and stored gas in gas storage *gs* at time *t*
$GL_{l,t}$	Gas load *L* at time *t*
$GW_{g,t}$	Supplied gas by the gas supplier g at time *t*
$\pi_{m,t}$	Natural gas pressure in node *m* at time *t*
$F_{pl,t}$	Natural gas flow of the line *pl* at time *t*
SU_{i}, SD_{i}	Start-up and shut-down cost of the non-gas-fired unit *i*
SUG_{i}, SDG_{i}	Start-up and shut-down fuel consumption of the gas-fired unit *i*
$\delta_{b,t}$	Angle of the power system bus *b* at time *t*

1. Introduction

1.1 Motivation

The interdependency among various energy carriers has attained a great of importance in energy systems by restructuration of such systems. The integrated energy systems including renewable/non-renewable energy sources [1, 2], gas-fired and thermal plants, combined heat and power (CHP) units and energy storage technologies have significant importance in increasing the efficiency of energy systems [3-5]. The most important advantage of integrated energy systems is the utilization of alternative energy sources for supplying different kinds of energy demands. On the other hand, separate optimization of energy systems operation does not verify the whole optimal operation of systems since the systems operate without considering the interdependent energy carriers.

A large source of electricity generation, which is one of the main elements of economic and social improvements, is oil, gas, and coal. In traditional studies, the operation of electricity and gas networks was accomplished separately; however, these two networks are interconnected, and each network has a significant effect on the other one. The integration of electricity and gas networks is increasing due to the increment of gas-fired CHP units, gas-fired non-CHP units, and power-to-gas technologies. The main advantages of gas-fired generation plants with respect to thermal plants are lower generation cost and pollutant gas emissions and high response speed to the variation of renewable power. The reported statistics verify the extension of integrated gas and electricity networks. In the United States, the consumption of natural gas to generate power has been increased from 27% in 2007 to 39% in 2009. A similar report shows an increment of natural gas consumption for power generation from 15% in 2000 to more than 50% in 2014 [6].

In addition, cogeneration of heat and power in industrial, commercial and residential sections can

be introduced as practical integrated energy systems, which utilizes CHP plants, boilers, and district heating networks (DHN) to supply the power and heat demands [7, 8]. CHP plants are one of the significant technologies for supplying power and heat demands, which are able to increase the efficiency of power generation to 90%, and decrease the emission of pollutant gases almost 13-18% [9]. Moreover, DHN, which are systems to distribute generated heat in a central point to supply industrial and residential heat demands, are practical instances of integrated power and heat networks. Accordingly, DHN integrates electricity and heat networks by connecting to CHP units, boilers and heat pumps. Such systems are effective in reducing the emission of pollutant gases and decreasing dependency on fossil fuels. To this end, in this paper, the effect of multi-carrier energy storage systems coordinated with wind power is investigated under an integrated framework called multi-network constrained unit commitment (UC), in which the constraints related to power, gas, and district heating networks are modeled by details.

1.2 Literature review

Recently, remarkable studies have been concentrated on integrated electricity and gas networks. In [10], the security-constrained operation of integrated electricity and gas networks has been studied considering the consequences of both networks such as disruptions in gas pipelines and power transmission losses. To improve the whole network operation, the optimal coordinated operation of such networks is proposed in [11] considering the uncertainties of wind power generation. In addition, an incentive-based demand response program is introduced for both networks to adjust electricity and gas demands. The authors have studied an energy flow model for electricity and gas networks in [12] using the Newton–Raphson approach to solve the problem. In [3], robust operation of electricity and gas networks has been proposed considering power-to-gas technology and the effect of the integrated network in adjusting the power demand. The

expansion planning of integrated electricity and gas networks has been studied in [13] using an integrated mixed-integer linear programming, which is able to reduce the number of binary and continues variables of the problem. A bi-level model for the optimal operation of such networks has been proposed in [14] in order to minimize the operation cost of the integrated network and maximize the profit of private owners. The authors have introduced a bi-level model for handling the optimal operation of an electricity network in the upper-level and supplying the gas network in a lower-level in [15]. A multi-objective model has been studied for optimal operation of integrated electricity and gas networks considering power to gas technology in [16], where two competing objectives are considered including the reduction of cost and gas emissions. The authors have studied bi-level planning of integrated gas and electricity networks in [17] considering power-to-gas technology, where the upper and lower levels challenge the expansion planning and obtaining optimal economic dispatch, respectively. Operation management of an integrated gas and electricity network has been addressed in [18] considering the linear representation of the constraints in the gas network together with demand response program and load demand uncertainty. Likewise, in [19], an approximate linear method has been proposed for modeling the non-linear limitations of the gas network. In [20], a two stage stochastic co-optimization problem of joint energy and reserve has been investigated in coordinated electricity and gas networks. A non-probabilistic model for optimal scheduling of coordinated power and gas networks has been proposed in [21], where the compressed air energy storage is included to reduce the operation cost of the power system. In [22], a robust approach has been presented for the integrated power and gas systems, where the power line outage is considered as the uncertain parameter. The authors have proposed a two-stage robust optimization problem for integrated power and gas systems in [23], where the uncertainties of both networks are considered.

In [24] a network-constrained UC problem for the coordinated power and district heating networks has been studied, where the thermal storage has been introduced as a flexible technology to reduce the total operation cost. The authors have studied a network-constrained UC problem for integrated heat and power networks in the presence of CHP plants and DHN in [25], where heat energy storage technology is considered for managing the variability of wind power generation. In the same work, the temperature variation of water flowing in the DHN and the effect of heat storage in the flexibility of the networks have been investigated. In [26], the optimal operation of integrated heat and power systems has been analyzed considering risk index for dealing with uncertainties of power market price and power generation of wind turbines. In this literature, the constraints of power and heat have not been considered. A robust scheme has been proposed for optimal scheduling of integrated heat and power networks in [9] for modeling the uncertainties associated with power market price and load demand. In [27], a multi-objective model has been introduced for optimal operation of integrated heat and power networks handling two conflicting objectives including minimization of operation cost and pollutant gas emission. The seasonal autoregressive integrated moving average model has been adopted in [28] for studying the scheduling of integrated heat and power networks considering the uncertainties of wind power production, load demand, and power market price. Similar research has been accomplished in [29] proposing real-time scheduling for demand-side management using real-time power market signals for the price. Bi-level optimal power flow is proposed for heat and power networks in [30], where profit maximization of the network and CHP plant owner are considered in the upper-level and lower-level, respectively. An optimal operation model for integrated heat and power networks has been proposed in [31] without taking uncertainties and gas network into account. A deterministic network-constrained economic dispatch model has been investigated for integrated electricity and

heat networks in [32] without considering the uncertainties associated with power system parameters such as wind power production. A focus has been given to the area of integrated electricity, gas and heat networks in the literature. In [33], the authors have proposed an optimal power flow framework for gas, electricity and district heating systems without multi-carrier energy storage technologies and uncertain parameters. Similar network-constrained power flow models have been proposed in [34] and [35], where uncertain parameters and multi-carrier energy storage have not been studied. An energy management model for multi-carrier microgrid has been presented in [36], where the network constraints of electricity, gas, and district heating systems have been ignored. Energy flow in integrated gas, electricity and heat networks has been studied in [37] considering uncertain parameters implementing a scenario-based model. In this literature, the constraints related to natural gas and district heating networks have been simply modelled without a detailed focus on the network constraints and an interconnecting component of the integrated system.

In the reviewed articles above, a robust optimization method or scenario-based approach has been applied mainly for modeling uncertain parameters, and the impact of information gap-decision theory (IGDT) on integrated electricity, gas and heat systems is not investigated. IGDT is defined as an uncertainty-handling method to deal with severe uncertain parameters, which takes advantage of the elimination of requiring probability distribution function unlike other uncertainty handling techniques such as Monte Carlo simulation approach [38]. Moreover, the maximum radius of the uncertain parameter is not required to be determined by IGDT that is effective in finding different strategies for the user. The major objective of the IGDT is providing a maximum uncertainty radius for the uncertain parameter by satisfying the objective function in a predetermined interval. IGDT is a high-performance uncertainty-handling method in energy

systems problems, which is applied to study problems in the area of optimal operation of distribution network [39], energy and frequency studies of micro-grids [40], energy management of smart buildings [41] and UC problem [42, 43].

1.3 Contribution

In none of the previous literature, interdependency between power, gas and heating networks has been considered simultaneously. Table 1 represents the contributions of the proposed model compared to the existing literature. The purpose of solving the traditional network-constrained UC problem is to minimize the operation cost of the power system considering the limits of the electricity network while the constraints of other energy networks are ignored. Literature has developed mainly the traditional network-constrained UC problem for coordinated operation of power and gas networks, or power and heating networks, where the interdependency between all three networks has been ignored. The pressure drop in the natural gas system and increasing heat loss in the district heating system by an increase of gas and heat loads in winter can make an important problem for sharing the produced heat and power by gas-fired based CHP units to supply demand. By increasing heat losses, CHP units need to generate more heat, as a result, the gas used by these units increases. On the other hand, residential gas loads have a higher priority to receive gas fuel compared to gas demand for gas-fired units. In addition, in previous literature, the effect of multi-carrier energy storage systems on the operation of the integrated power, natural gas and district heating networks under a UC problem with wind energy has not been examined. To respond to these challenges, the present work proposes a multi-network constrained UC problem based on the IGDT method considering the multi-carrier energy storage technologies integrated with wind energy as well as constraints of gas, electricity, and district heat network, which is shown in Fig. 1. The most important contributions of this work can be summarized as follows:

- Solving electricity, gas, and district heating networks-constrained UC problem based on the IGDT approach, where the effect of residential gas load variations, gas system pressure limits, and loss of the DHN on the total operation cost and hourly dispatch of the plants are investigated.
- Considering the multi-carrier energy storage technologies in the coordinated systems as a practical option for decreasing the total operation cost of the system and reducing the effect of wind power uncertainty on operation cost of the integrated network.
- Modeling the uncertainty of wind power generation under risk-seeker and risk-averse strategies in multi-carrier energy networks using an IGDT-based approach without needing the probability distribution function or fuzzy members.
- Proposing an simple concept for converting the bi-level problem to a single-level one in the integrated systems without using Karush–Kuhn–Tucker (KKT) conditions.

Table 1: Comparison between the proposed model and other presented works

Ref	UC problem	Modeling network constraints			Energy storage systems			Modeling the uncertain parameter
		Electricity	Gas	District Heating	Power	Gas	Thermal	
[6]	■	■	■					Stochastic
[11]	■	■	■			■		Interval
[16]	■	■	■					Two-stage stochastic
[18]	■	■	■		■			Two-stage stochastic
[21]	■	■	■		■			Robust
[22]	■	■	■			■		Robust
[23]	■	■	■			■		Two-stage robust
[24]	■	■		■			■	Deterministic
[25]	■	■		■			■	Two-stage robust
[42]	■							IGDT
[43]	■	■			■			IGDT
Proposed model	■	■	■	■	■	■	■	IGDT

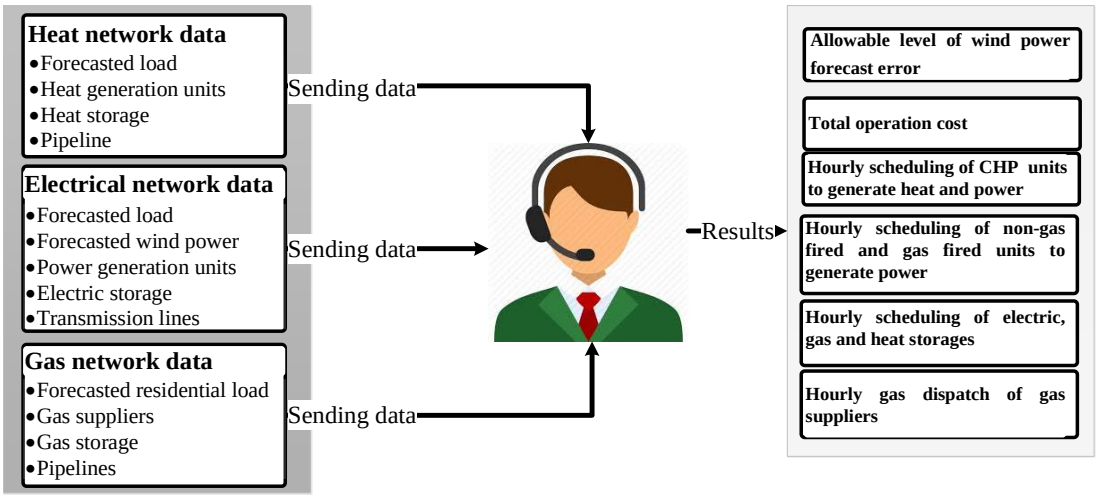

Fig. 1. Schematic diagram of the proposed model

2. Problem formulation

In this section, the formulation of the proposed model for integrated electricity, gas and heat network is provided, and the constraints of each network as well as the interconnecting elements as shown in Fig. 2 are investigated.

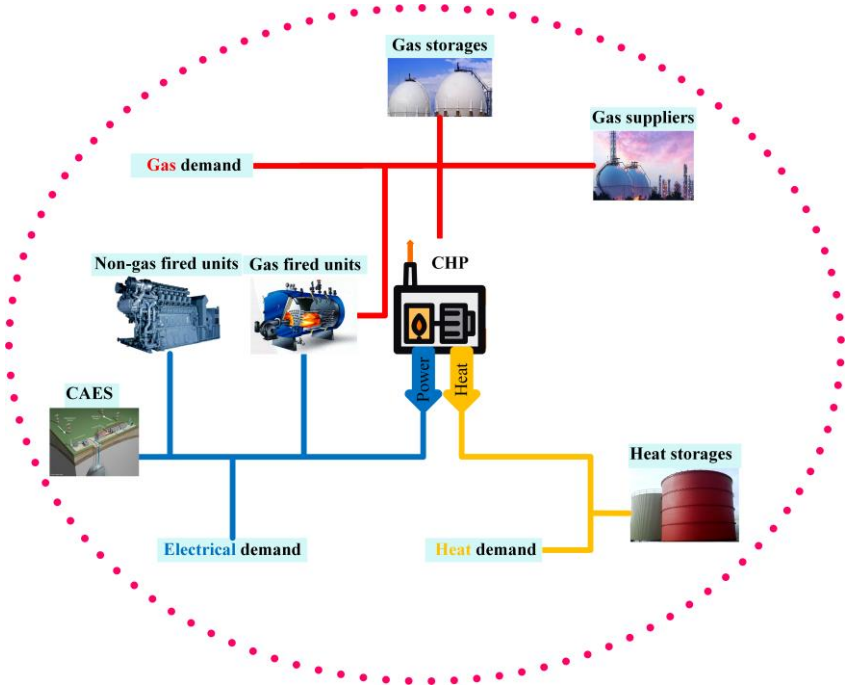

Fig. 2. The interconnection in multi-carrier energy systems

2.1. Objective function

The main objective of the proposed model is to minimize the operation cost of the integrated electricity, gas and heat networks, which is defined as (1). The first term of the objective function is related to the cost of power generation and start-up and shut-down of the non-gas-fired units. The second term is related to the variable costs of the power storage unit. Also, the third term is the natural gas supply by the gas suppliers, and the last term is related to the operation cost of the gas storage unit. It should be noted that the cost of the gas-fired plants (i.e., CHP and only-power units) and power storage in discharge mode is considered in the third term since the fuel of such units is natural gas. Power storage studied in this paper is compressed air energy storage (CAES) with fuel consumption of natural gas in discharge mode.

$$OF = Min\sum_{t=1}^{NT}\left[\begin{array}{l}\sum_{i=1}^{NE}\left[F\left(P_{i,t}\right)+SU_{i,t}+SD_{i,t}\right]+\sum_{e=1}^{NSE}\left[P_{e,t}^{D}VOM^{\exp}+P_{e,t}^{C}VOM^{c}\right]\\+\sum_{g=1}^{NGW}\rho^{gas}GW_{g,t}+\sum_{gs=1}^{NGS}C_{s}GS_{gs,t}^{out}\end{array}\right] \quad (1)$$

2.2. Unit commitment constraints

It should be mentioned that the power and heat generated by the CHP units have a mutual dependency. In other words, each CHP unit can be operated only in the feasible operating region (FOR), which is shown in Fig. 3. Generation plants have capacity limitation constraints including the power generation capacity and FOR of the CHP units as follows [29]:

$$P_i^{\min} I_{i,t} \le P_{i,t} \le P_i^{\max} I_{i,t} \quad (2)$$

$$P_{i,t} - P_i^A - \frac{P_i^A - P_i^B}{H_i^A - H_i^B} \times (H_{i,t} - H_i^A) \le 0 \quad i \in NC \quad (3)$$

$$P_{i,t} - P_i^A - \frac{P_i^A - P_i^B}{H_i^A - H_i^B} \times (H_{i,t} - H_i^A) \le 0 \quad i \in NC \tag{4}$$

$$P_{i,t} - P_i^B - \frac{P_i^B - P_i^C}{H_i^B - H_i^C} \times (H_{i,t} - H_i^B) \ge -(1 - I_{i,t}) \times M \quad i \in NC \tag{5}$$

$$P_{i,t} - P_i^C - \frac{P_i^C - P_i^D}{H_i^C - H_i^D} \times (H_{i,t} - H_i^C) \ge -(1 - I_{i,t}) \times M \quad i \in NC \tag{6}$$

$$0 \le H_{i,t} \le H_i^A \times I_{i,t} \quad i \in NC \tag{7}$$

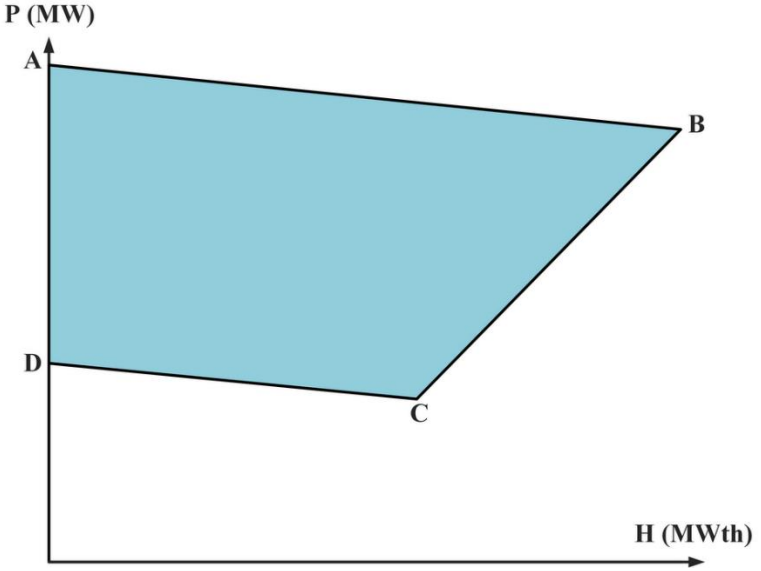

Fig. 3. FOR of the CHP plant

Ramp rate limitations are considered for modeling the effect of ramp-up/down limitations at consecutive periods. In addition, the minimum up/downtime limitations of the generation plants should be considered as follows [22]:

$$P_{i,t} - P_{i,t-1} \le \left[1 - I_{i,t}(1 - I_{i,t-1})\right] R_i^{up} + I_{i,t}(1 - I_{i,t-1}) P_i^{\min} \tag{8}$$

$$P_{i,t-1} - P_{i,t} \le \left[1 - I_{i,t-1}(1 - I_{i,t})\right] R_i^{dn} + I_{i,t-1}(1 - I_{i,t}) P_i^{\min} \tag{9}$$

$$(X_{i,t-1}^{on} - T_i^{on})(I_{i,t-1} - I_{i,t}) \ge 0 \tag{10}$$

$$(X_{i,t-1}^{off} - T_i^{off})(I_{i,t} - I_{i,t-1}) \geq 0 \quad (11)$$

The start-up and shut-down cost of the non-gas-fired generation plants is considered as (12)-(13). Moreover, the fuel consumption of the gas-fired plants in start-up and shut-down times are studied as (14)-(15) as follows [22]:

$$SU_{i,t} \geq su_i (I_{i,t} - I_{i,t\text{-}1}) \quad i \in NE \quad (12)$$

$$SD_{i,t} \geq sd_i (I_{i,t\text{-}1} - I_{i,t}) \quad i \in NE \quad (13)$$

$$SUG_{i,t} \geq sug_i (I_{i,t} - I_{i,t\text{-}1}) \quad i \in NGC \quad (14)$$

$$SDG_{i,t} \geq sdg_i (I_{i,t\text{-}1} - I_{i,t}) \quad i \in NGC \quad (15)$$

2.3. Electrical storage constraints

In this paper, the CAES system is considered in the power network for storing the power at off-peak hours and discharge the power at on-peak hours, which is modeled as (16)-(21). This type of storage compresses the air using electricity when the power cost is low. Next, the compressed air is stored in a salty dome-shaped space. In periods of high power cost, this technology can use compressed air to generate power. Hence, there is no need for extra gas to compress air. In fact, the consumed gas by a simple cycle gas-turbine is twice the gas used by CAES to generate power. Accordingly, with respect to the features mentioned, CAES can be introduced as a suitable option for the system operator to reduce the operating cost of the integrated energy system. Fig. 4 describes the method of energy generation by a simple type of CAES. The CAES can be operated in one of the ideal/charge/discharge modes, which is denoted in (16). The charge and discharge power of the CAES is limited to its minimum and maximum amounts by (17) and (18). The relation

between stored air at the CAES and power charge and discharge of the unit is satisfied by (19). The limitation of stored air in the CAES and initial and final stored air is studied by (19)-(21).

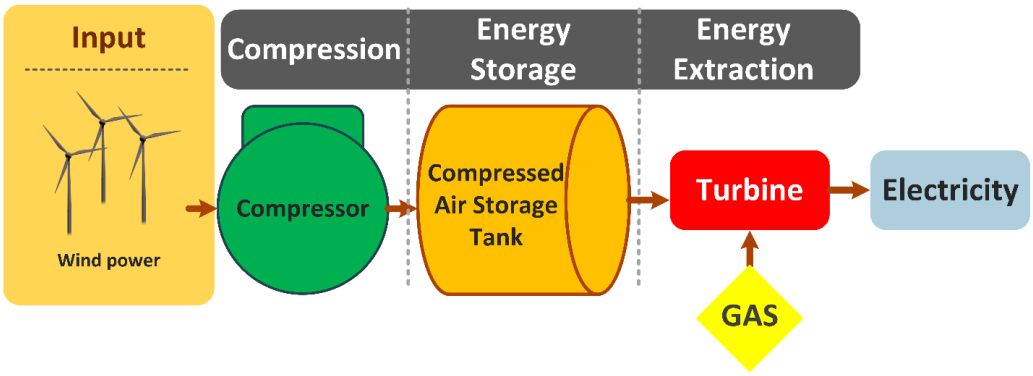

Fig. 4. mehod of energy storage and generation of CAES

$$I_{e,t}^{C} + I_{e,t}^{D} \leq 1 \tag{16}$$

$$P_{e}^{C,\mathrm{Min}}\, I_{e,t}^{C} \leq P_{e,t}^{C} \leq P_{e}^{C,\mathrm{Max}}\, I_{e,t}^{C} \tag{17}$$

$$P_{e}^{D,\mathrm{Min}}\, I_{e,t}^{D} \leq P_{e,t}^{D} \leq P_{e}^{D,\mathrm{Max}}\, I_{e,t}^{D} \tag{18}$$

$$A_{e,t} = A_{e,t\text{-}1} + \eta_{e}^{C} P_{e,t}^{C} - \frac{P_{e,t}^{D}}{\eta_{e}^{D}} \tag{19}$$

$$A_{e}^{\min} \leq A_{e,t} \leq A_{e}^{\max} \tag{20}$$

$$A_{e,0} = A_{e,in} \tag{21}$$

$$A_{e,0} = A_{e,NT} \tag{22}$$

2.4. Thermal storage constraint

A water-based sensible thermal storage has been used in the district heating network under temperature 100 °C to meet demand. The heat stored in the thermal storage unit is variable in the

scheduling time horizon, which is mentioned in (23) considering heat loss. Equation (24) denotes the limitation of energy stored in the thermal storage unit. In addition, the limitations of the charge and discharge of the thermal storage unit are satisfied by (25)-(26).

$$B_{hs,t} = (1-\eta_{hs})B_{hs,t-1} + \eta_{hs}^{ch} HS_{hs,t}^{ch} - \frac{HS_{hs,t}^{dis}}{\eta_{hs}^{dis}} - \beta_{\text{loss}} SU_{hs,t} + \beta_{\text{gain}} SD_{hs,t} \tag{23}$$

$$B_{hs}^{\text{Min}} \le B_{hs,t,s} \le B_{hs}^{\text{Max}} \tag{24}$$

$$B_{hs,t} - B_{hs,t-1} \le B_{hs}^{\text{Max, charge}} \tag{25}$$

$$B_{hs,t-1} - B_{hs,t} \le B_{hs}^{\text{Max, discharge}} \tag{26}$$

2.5. Gas storage constraints

The gas storage system is studied in the integrated system in this paper as a practical solution when the gas load cannot be supplied. Equations (27) and (28) formulate the limitation of the storage and release of the storage unit. Moreover, (29) and (30) formulates the storage balance and capacity limits. In addition, the initial and final conditions of storage are satisfied by (31) and (32).

$$0 \le GS_{gs,t}^{out} \le GS_{gs,\max}^{out} \tag{27}$$

$$0 \le GS_{gs,t}^{in} \le GS_{gs,\max}^{in} \tag{28}$$

$$E_{gs,t} = E_{gs,\,t\text{-}1} + \eta_{gs}^{in} GS_{gs,t}^{in} - \frac{GS_{gs,t}^{out}}{\eta_{gs}^{out}} \tag{29}$$

$$E_{gs}^{\min} \le E_{gs,t} \le E_{gs}^{\max} \tag{30}$$

$$E_{gs,0} = E_{gs,\text{intial}} \tag{31}$$

$$E_{gs,0} = E_{gs,end} \tag{32}$$

2.6 Electrical network constraints

The power balance of the electricity networks determines the balance between the power generation of plants and load demand. In addition, the power flow between the electricity network buses is considered linear, which should be limited to its lower and upper bounds:

$$\sum_{i=1}^{NU_b} P_{i,t} + \sum_{e=1}^{NES_b} \left(P_{e,t}^{D} - P_{e,t}^{C} \right) + \sum_{wf=1}^{NWf_b} P_{wf,t} - \sum_{j=1}^{NJ_b} D_{j,t} = \sum_{L=1}^{NL_b} PF_{L,t} \tag{33}$$

$$PF_{L,t} = \frac{\delta_{b,t} - \delta_{b',t}}{x_L} \tag{34}$$

$$-PF_L^{max} \le PF_{L,t} \le PF_L^{max} \tag{35}$$

2.7. District heating network constraints

The mass flow balance in the heat network should be considered as (36). For each node *h*, a positive mass flow rate defined as the inflow and negative mass flow rate is defined as the outflow.

$$\sum_{i=1}^{NC_h} HQ_{i,t} + \sum_{hs=1}^{NHS} (HDQ_{hs,t} - HSQ_{hs,t}) - \sum_{hl=1}^{NHL_h} HLQ_{hl,t} = \sum_{hp=1}^{NHP_h} HP_{hp,t} \tag{36}$$

The relation between mass flow and heat energy can be stated as follows for heat load and heat source, respectively. Equations (38) and (39) define the generated heat and stored heat in the heat storage in terms of mass flow rate [31].

$$HQ_{i,t} \times (T_{h,t} - T_{h,t}^{back}) \times c - 3600 \times H_{i,t} = 0 \;\; i \in NC \tag{37}$$

$$HDQ_{hs,t} \times (T_{h,t} - T_{h,t}^{back}) \times c - 3600 \times HD_{hs,t}^{dis} = 0 \tag{38}$$

$$HCQ_{hs,t} \times (T_{h,t} - T_{h,t}^{back}) \times c - 3600 \times HS_{hs,t}^{ch} = 0 \tag{39}$$

$$HLQ_{hl,t} \times (T_{h,t} - T_{h,t}^{back}) \times c - 3600 \times HL_{hl,t} = 0 \quad (40)$$

A temperature drop of the hot water is a function of mass flow, length and heat loss coefficient of the line, which can be obtained as (41). Heat loss coefficient can be determined using the water temperature in the pipeline, the environment temperature and resistance of the channel and insulation material as follows [31]:

$$\Delta T_{hP,t} = \frac{3.6 \times k_{hp} \times (1+\beta) \times Le_{hp}}{1000 \times c \times HP_{hp,t}} \quad (41)$$

$$k_{hp} = \frac{T_{hp} - T_0}{R_1 + R_2} \quad (42)$$

The water temperature of each heat node should be limited to its minimum and maximum values (43). The capacity limitation of the water flow of each heat line should be considered as (44).

$$T_h^{\min} \le T_{h,t} \le T_h^{\max} \quad (43)$$

$$HP_{hp}^{\min} \le HP_{hp,t} \le HP_{hp}^{\max} \quad (44)$$

2.8. Gas network constraints

The natural gas flow through line *pl* without compressors is formulated as a quadratic function of the two end nodes pressures as (45)-(46). The natural gas flow through line *pl* considering compressors is stated in (47), where the gas flow capacity of the gas pipeline will be increased. Gas nodes have pressure limitation constraints as (48). Gas suppliers have capacity limitation for providing the nodal gas demands as (49). Natural gas end-users in this model contain the residential gas loads and gas-fired generation units (i.e., CHP, power-only units and CAES). Natural gas loads should be limited to its lower and upper bounds (50). The gas balance of the gas networks verifies

the balance between the gas provided by gas supplies and gas consumption as (51) [22]:

$$F_{pl,t} = \text{sgn}(\pi_{m,t}, \pi_{n,t})\, C_{m,n} \sqrt{\left|\pi_{m,t}^2 - \pi_{n,t}^2\right|} \tag{45}$$

$$\text{sgn}(\pi_{m,t}, \pi_{n,t}) = \begin{cases} 1 & \pi_{m,t} \geq \pi_{n,t} \\ -1 & \pi_{m,t} \leq \pi_{n,t} \end{cases} \tag{46}$$

$$F_{pl,t} \geq \text{sgn}(\pi_{m,t}, \pi_{n,t})\, C_{m,n} \sqrt{\left|\pi_{m,t}^2 - \pi_{n,t}^2\right|} \tag{47}$$

$$\pi_m^{\min} \leq \pi_{m,t} \leq \pi_m^{\max} \tag{48}$$

$$GW_g^{\min} \leq GW_{g,t} \leq GW_g^{\max} \tag{49}$$

$$GL_l^{\min} \leq GL_{l,t} \leq GL_l^{\max} \tag{50}$$

$$\sum_{g=1}^{NGW_m} GW_{g,t} + \sum_{gs=1}^{NGS_m} \left(GS_{gs,t}^{out} - GS_{gs,t}^{in}\right) - \sum_{gl=1}^{NGL_m} GL_{gl,t} = \sum_{pl=1}^{NPL_m} F_{pl,t} \tag{51}$$

2.9. Coupling constraints for integrated networks

The natural gas fuel consumption of the CHP units (kcf) is a function of generated heat and power, which can be stated as (52). Similarly, the natural gas fuel consumption of the power-only plants is a function of producing power, which can be stated as (53). Each gas supply amount for providing the natural gas fuel CAES is a natural gas load of the gas network, which can be mentioned by (54). CHP units and power-only units are considered as large consumers of the natural gas network, which are connected to the gas network as natural gas loads as (55)-(57).

$$F_{i,t}^{CHP} = c_i + b_i P_{i,t} + a_i (P_{i,t})^2 + + d_i H_{i,t} + e_i (H_{i,t})^2 + f_i H_{i,t} P_{i,t} + SUG_{i,t} + SDG_{i,t} \quad i \in NC \tag{52}$$

$$F_{i,t}^{G} = c_i + b_i P_{i,t} + a_i \left(P_{i,t}\right)^2 + SUG_{i,t} + SDG_{i,t} \quad i \in NG \tag{53}$$

$$F_{e,t} = HR_e P_{e,t}^D \quad (54)$$

$$GL_{gl,t} = F_{i,t}^{CHP} \quad \forall gl = i,...,NC \quad (55)$$

$$GL_{gl,t} = F_{i,t}^{G} \quad \forall gl = i,...,NG \quad (56)$$

$$GL_{gl,t} = F_{e,t} \quad \forall gl = e,...,NES \quad (57)$$

3. The problem formulation based on IGDT approach

In this paper, an IGDT-based method is applied for modelling the uncertainty of wind power in multi-network constrained UC. IGDT is an effective approach to assess and analyze the strategies used at times of uncertainty, and the operator would be ready to determine the effectiveness of each strategy based on the defined priorities and objective functions. The proposed model is defined as a bi-level optimization method. Bi-level problem is described as a mathematical problem, where an optimization problem includes another optimization problem as a constraint [44]. Solving a bi-level problem is hard by applying available solvers. The method of Lagrange Multipliers is used for achieving the optimal solution of a problem constrained to one or more equalities. The model must be extended to the KKT conditions when the problem equations also have inequalities. In other words, the objective function $F(x)$ is minimized regarding all equalities $h_i(x) = 0$ and all inequalities $g_k(x) \leq 0$. The inequality conditions are added to the Lagrange Multipliers method regarding the objective function as well as the constraints in a single minimization problem, where the equality constraint by a factor i and the inequality constraints by a factor k are known as the KKT multipliers [9]. As a result, the proposed IGDT-based technique can be converted to a single level problem applying KKT conditions. however, in this paper an innovative approach is applied to make a single-level problem. IGDT has several advantages

compared to the scenario-based modeling method and robust optimization approach, which can be classified as follows:

1. The IGDT approach, unlike the scenario-based programming, does not require a probability distribution function to model the uncertain parameter of the problem.

2. In scenario-based approaches, problem-solving time is increased due to the production of a large number of scenarios. However, the calculation time of the problem using the IGDT approach is decreased due to the absence of the scenarios.

3. Compared to the robust optimization method that considers only one risk-averse approach for an uncertain parameter, the IGDT approach considers two risk-averse and risk-seeker strategies that increase the decision-making range of the network operator.

In the following, the formulation of the IGDT approach is expressed in detail.

3.1. IGDT based problem formulation

The mathematical description of the uncertainty of the problem is defined as (58), where the predicted value of the parameter is indicated by $\bar{\Psi}$. Moreover, ε is the maximum possible deviation of an uncertain parameter from its prediction value, which is called the unknown uncertainty radius for the decision-maker [44].

$$U = U(\bar{\Psi}, \varepsilon) = \left\{ \Psi : \left| \frac{\Psi - \bar{\Psi}}{\bar{\Psi}} \right| \leq \varepsilon \right\} \tag{58}$$

In the IGDT approach, the risk-averse and risk-seeker strategy are considered, which are demonstrated in Fig. 5. Equations (59) and (60) defines the mathematical model of these two

strategies, where Δ_C and OF_b are the critical value and the base value of the objective function, respectively. Also, x is the decision variable of the problem. E_r is defined as a cost deviation factor that models the maximum cost accepted by the operator. E_p is expressed as a cost deviation factor that models the minimum cost desired by the operator [44].

$$\alpha(X,\Delta_C)=Max\left\{\varepsilon:\left(\underset{\Psi\in U(\bar{\Psi},\varepsilon)}{Max}\ OF\le\Delta_C=(1+E_r)OF_b\right)\right\} \tag{59}$$

$$\beta(X,\Delta_C)=Min\left\{\varepsilon:\left(\underset{\Psi\in U(\bar{\Psi},\varepsilon)}{Min}\ OF\le\Delta_C=(1-E_\rho)OF_b\right)\right\} \tag{60}$$

In the risk-averse strategy, the uncertain parameter causes an undesirable effect on the objective function. Therefore, the system operator takes into account a higher cost associated with the undesirable deviation of wind power in this strategy, which is given by (61)-(64) as a bi-level problem.

$$\alpha=Max\ \varepsilon \tag{61}$$

$$Max\sum_{t=1}^{NT}\left[\begin{array}{l}\sum_{i=1}^{NE}\left[F\left(P_{i,t}\right)+SU_{i,t}+SD_{i,t}\right]+\sum_{e=1}^{NSE}\left[P_{k,t}^{D}VOM^{\exp}+P_{k,t}^{C}VOM^{c}\right]\\+\sum_{g=1}^{NGW}\rho^{gas}GW_{g,t}+\sum_{gs=1}^{NGS}C_sGS_{gs,t}^{out}\end{array}\right]\le\Delta_C \tag{62}$$

$$(1-\varepsilon)\bar{P}_{wf,t}\le P_{wf,t}\le(1+\varepsilon)\bar{P}_{wf,t} \tag{63}$$

(2)-(57) (64)

In the risk-seeker strategy, the network operator solves the multi-network constrained UC problem under a lower operation cost due to a desirable deviation of wind power production from its predicted value, which is a bi-level problem indicated by (65)-(68).

$$\beta = Min\ \varepsilon \tag{65}$$

$$Min \sum_{t=1}^{NT} \left[\begin{array}{l} \sum_{i=1}^{NE} \left[F\left(P_{i,t}\right) + SU_{i,t} + SD_{i,t} \right] + \sum_{e=1}^{NSE} \left[P_{k,t}^{D} VOM^{\exp} + P_{k,t}^{C} VOM^{c} \right] \\ + \sum_{g=1}^{NGW} \rho^{gas} GW_{g,t} + \sum_{gs=1}^{NGS} C_s GS_{gs,t}^{out} \end{array} \right] \leq \Delta_C \tag{66}$$

$$(1-\varepsilon)\,\bar{P}_{wf,t} \leq P_{wf,t} \leq (1+\varepsilon)\,\bar{P}_{wf,t} \tag{67}$$

(2)-(57) (68)

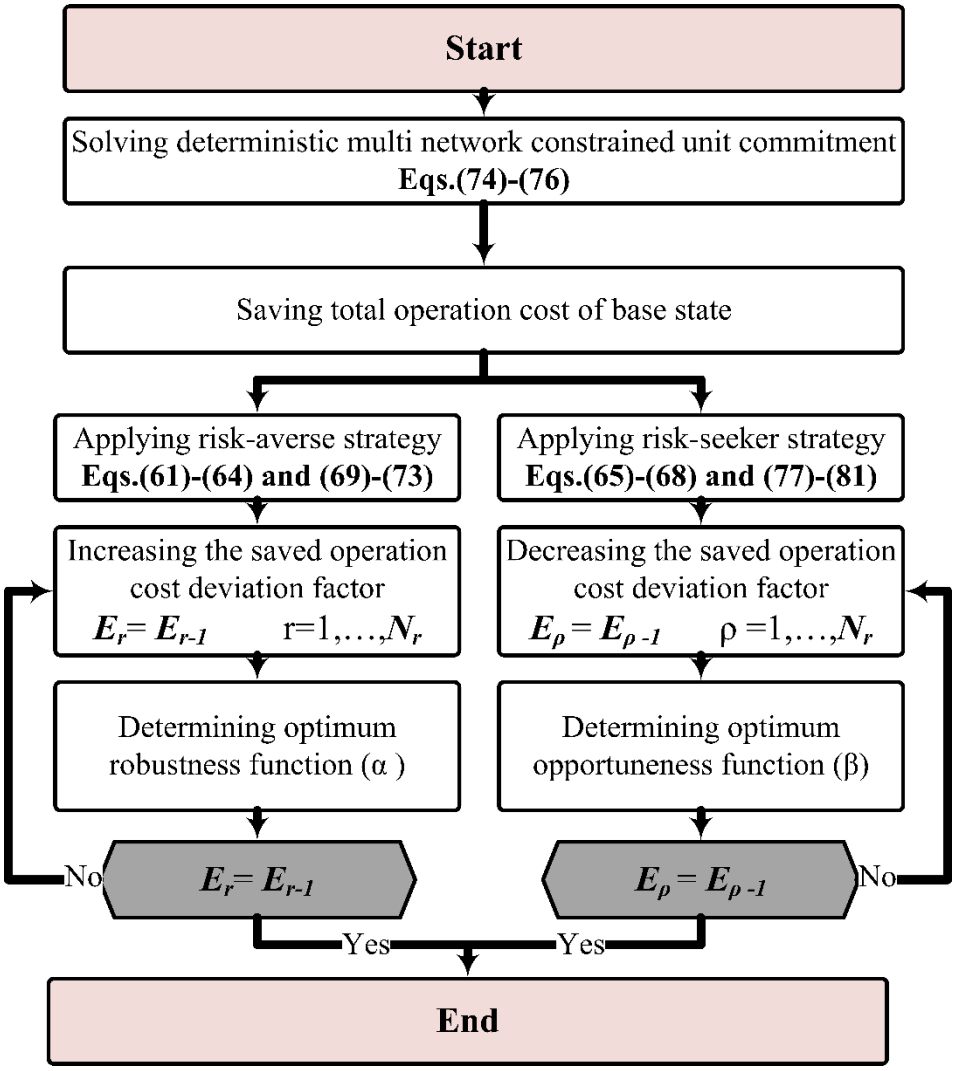

Fig. 5. The flowchart of the proposed IGDT approach

3.2. Single-level formulation

The proposed bi-level optimization problem is transformed into a single-level problem for solving by common solvers in both the risk-averse and risk-seeker strategy, which is stated in the following.

3.2.1. Robustness function

As stated before, the forecast error in power generation in the risk-averse strategy is modeled in a way that increases the operation cost. Therefore, in this strategy, only a reduction in wind power has an undesirable effect on the operation cost of the system. As a result, the bi-level problem given in (61)-(64) can be converted into a single- level problem as follows.

$$\alpha = Max\ \varepsilon \tag{69}$$

$$\sum_{t=1}^{NT}\left[\begin{array}{l}\sum_{i=1}^{NE}\left[F\left(P_{i,t}\right)+SU_{i,t}+SD_{i,t}\right]+\sum_{e=1}^{NSE}\left[P_{k,t}^{D}VOM^{\exp}+P_{k,t}^{C}VOM^{c}\right]\\ +\sum_{g=1}^{NGW}\rho^{gas}GW_{g,t}+\sum_{gs=1}^{NGS}C_{s}GS_{gs,t}^{out}\end{array}\right]\leq\Delta_{C} \tag{70}$$

$$\Delta_{C}=(1+E_{r})OF_{b} \tag{71}$$

$$P_{wf,t}=(1-\varepsilon)\hat{P}_{wf,t} \tag{72}$$

(2)-(57) (73)

In (71), OF_b is the operation cost in the base state, which is formulated as (74)-(76). It is worth to note that multi-carrier energy storage systems are not considered in calculating the basic operation costs.

$$OF_b = \sum_{t=1}^{NT} \left[\begin{array}{l} \sum_{i=1}^{NE} \left[F\left(P_{i,t}\right) + SU_{i,t} + SD_{i,t} \right] + \sum_{e=1}^{NSE} \left[P_{k,t}^{D} VOM^{\exp} + P_{k,t}^{C} VOM^{c} \right] \\ + \sum_{g=1}^{NGW} \rho^{gas} GW_{g,t} + \sum_{gs=1}^{NGS} C_s GS_{gs,t}^{out} \end{array} \right] \quad (74)$$

$$P_{wf,t} = \hat{P}_{wf,t} \quad (75)$$

$$(2)-(15) \text{ and } (33)-(57) \quad (76)$$

3.2.2. Opportunity function

As discussed earlier, the uncertain parameter has a desirable effect on the operation cost of the system in the risk-seeker strategy. So, in this strategy, the optimal state occurs when wind power production increases with respect to its predicted value. Consequently, the bi-level problem given by (65)-(68) is converted to a one-level problem as follows.

$$\beta = Min\ \varepsilon \quad (77)$$

$$\sum_{t=1}^{NT} \left[\begin{array}{l} \sum_{i=1}^{NE} \left[F\left(P_{i,t}\right) + SU_{i,t} + SD_{i,t} \right] + \sum_{e=1}^{NSE} \left[P_{k,t}^{D} VOM^{\exp} + P_{k,t}^{C} VOM^{c} \right] \\ + \sum_{g=1}^{NGW} \rho^{gas} GW_{g,t} + \sum_{gs=1}^{NGS} C_s GS_{gs,t}^{out} \end{array} \right] \leq \Delta_C \quad (78)$$

$$\Delta_C = (1 - E_\rho) OF_b \quad (79)$$

$$P_{wf,t} = (1+\varepsilon)\, \hat{P}_{wf,t} \quad (80)$$

$$(2)\text{-}(57) \quad (81)$$

4. Numerical simulations

In order to evaluate the proposed model, an integrated electricity, gas, and heat network containing a 30-node heating system, a 6-node natural gas network, and a modified 6-node electric power

system is considered, which is shown in Fig. 6. Specifications related to 6-bus electricity and gas network are taken from [44] which descript an integrated energy system in transmission level [16, 21]. In addition, all data related to district heating network is given in [31], which shows an energy network model in the distribution level with radial structure [24, 25]. The forecasted energy demands and wind power are represented in Figs. 7 and 8. Capacity of the wind power plant is assumed to be 60 MW [21]. Data for power plants and multi-carrier energy storage systems is presented in Appendix 1 as Tables A1-A7 which all are collected from [20, 21, 31]. The maximum charge and discharge power of CAES are assumed to be 25MW, which covers about 30% power demand connected to bus 5 (CAES is located on this bus). The capacity of CAES is also considered 100 MWh, which provides 4 hours of full discharge capability for this storage. Besides, the maximum charge and discharge power of thermal storage are assumed to be 15MW, which considering heat losses, meets about 30% heat demand. The capacity of thermal storage is also considered 60 MWh, which provides 4 hours of full discharge capability. The price of natural gas is 2 $/kcf. The proposed problem is a mixed-integer non-linear programming problem that is solved by a DICOPT solver in the GAMS software. Four case studies have been investigated to evaluate the performance of the proposed model for integrated energy systems.

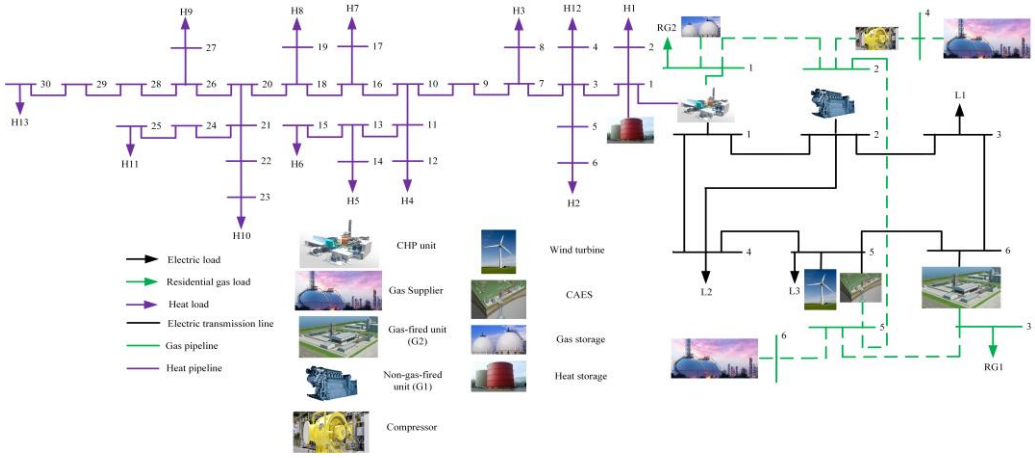

Fig. 6. The studied integrated electricity, gas and heating network

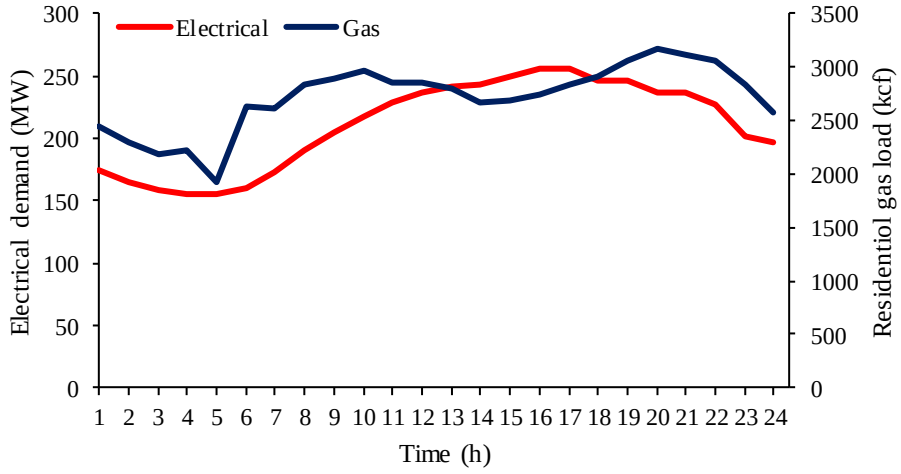

Fig. 7. The forecasted electrical and gas demand

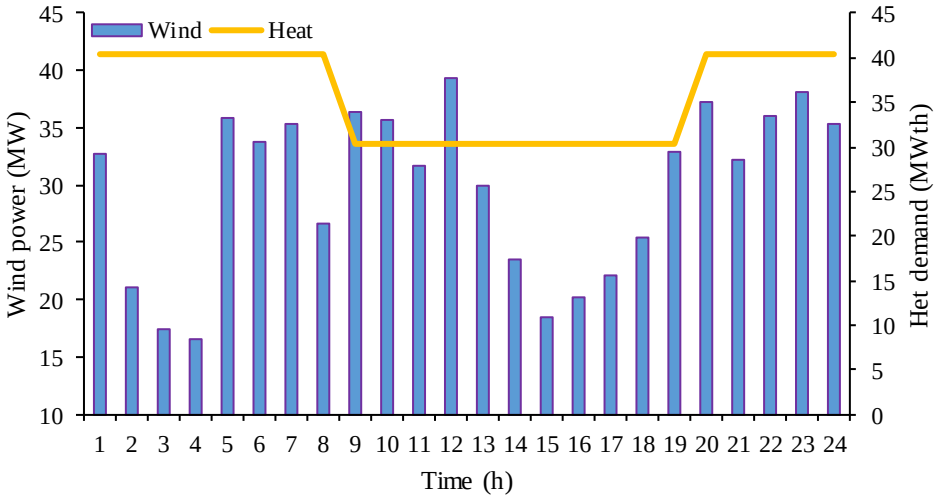

Fig. 8. The forecasted heat demand and wind power

Case 1: The main aim of this case is to concentrate on natural gas network constraints due to variations in residential gas loads. Figure 9 shows the effect of natural gas load variation on the pressure of nodes 1 and 3 of the natural gas system that contains the natural gas loads. As it can be observed from this figure, decrement or increment of the forecasted residential gas load has a significant impact on the pressures of such nodes in a way that the pressure of such nodes has been

decreased by increasing the forecasted gas load. The gas pressure in node 1 attained its minimum value by the increment of gas load demand (i.e., by 1.1 times of its forecasted value) between t=7 to t=24. Such a shortage of pressure can result in a shortage of transferring fuel to a CHP plant that is located at this node. The effect of natural gas load changes on the hourly dispatch of power plant production is given in Table 2. As can be predicted, the increase in natural gas load has resulted in declining the power generation capacity of the CHP plant, which has led to an increase in the participation of the G1 and G2 power plants in power demand-supply. It should be noted that due to the location of the G2 power plant in the natural gas network (i.e., node 3), this plant is not facing fuel shortage and it can produce power by its maximum capacity. The operation cost for various values of gas load demands is provided in Table 3, which demonstrates that the operation cost of integrated energy system has increased significantly by increasing natural gas load demand. This fact shows the interdependency of electricity and gas networks.

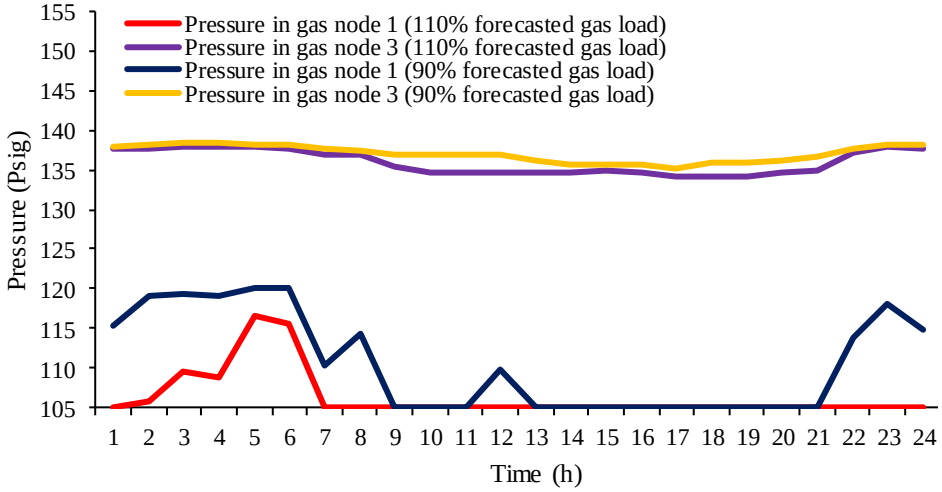

Fig. 9. Pressure changes in nodes of the gas system due to variations in residential gas load

Table 2. Hourly scheduling of units for different values of forecasted residential gas load

Time	90% forecasted gas load			100% forecasted gas load			110% forecasted gas load		
	CHP	G1	G2	CHP	G1	G2	CHP	G1	G2
1	142.410	0	0	142.410	0	0	142.41	0	0

2	144.090	0	0	144.090	0	0	144.09	0	0
3	141.290	0	0	141.290	0	0	141.29	0	0
4	138.150	0	0	138.150	0	0	138.15	0	0
5	123.236	0	0	119.220	0	0	119.22	0	0
6	126.780	0	0	126.780	0	0	126.78	0	0
7	138.110	0	0	138.110	0	0	138.11	0	0
8	163.720	0	0	163.720	0	0	163.72	0	0
9	169.160	0	0	169.160	0	0	147.497	11.663	10
10	181.520	0	0	181.520	0	0	137.466	20	24.054
11	196.890	0	0	186.890	0	10.000	137.466	20	39.424
12	196.820	0	0	196.820	0	0	147.497	20	29.323
13	200.963	0	11.357	199.479	0	12.841	147.497	20	44.823
14	200.963	0	19.117	199.479	10.000	10.601	147.497	20	52.583
15	200.963	10.000	19.417	200.963	10.000	19.417	157.529	20	52.851
16	200.588	14.922	20.000	199.479	16.031	20.000	147.497	20	68.013
17	200.963	12.877	20.000	172.120	41.720	20.000	117.403	20	96.437
18	200.963	10.000	10.377	172.120	29.220	20.000	117.403	20	83.937
19	200.963	0	12.107	172.120	20.950	20.000	117.403	20	75.667
20	190.110	0	10.000	180.074	10.000	10.036	127.18	20	52.93
21	195.150	0	10.000	195.150	0	10.000	157.275	20	27.875
22	191.060	0	0	191.060	0	0	191.06	0	0
23	0	0	0	0	0	162.950	0	0	0
24	0	0	0	0	0	161.390	0	0	0

Table 3. Operation cost for different values of forecasted gas load

	90% forecasted gas load	100% forecasted gas load	110% forecasted gas load
Total operation cost ($)	237294.09	259093.001	291724.55
Gas system operation cost ($)	232661.92	247364.608	242507.96
Power system operation cost ($)	4632.17	11728.393	41216.582

Case 2: In this case, the effect of district heating network constraints on the optimal scheduling of the integrated energy system is evaluated. Figure 10 shows the impact of considering heat losses on temperature drop at *t=6* and *t=12*. As it can be seen in this figure, the temperature has dropped from 1 to 30 in both time intervals, which is resulted from the dependency of heat losses to the mass flow rate and the length of the pipeline. In fact, the temperature has dropped from 100 °C in node 1 to 99.308 and 99.474 in node 30 at *t=6* and *t=12*. Also, the temperature drops in the *t=6* are more significant than *t=12*, which is due to the higher heat load at *t=6*. The effect of considering heat losses on the heat produced by the CHP power plant is depicted in Fig. 11. As it

can be seen in this figure, the CHP plant should generate more heat to meet the demand when heat losses are considered, which reduces the CHP electrical power generation and increase the participation of more expensive power plants in supplying electric power demand. In fact, the heat produced by the CHP power plant increased by 10% considering heat losses. Table 4 reports the dependency of electricity and natural gas networks on the heating system. As can be seen in this table, the total operation cost, the operation cost of the power system, and the operation cost of the gas system have been increased and power dispatch by the CHP power plant has decreased by considering the heat losses.

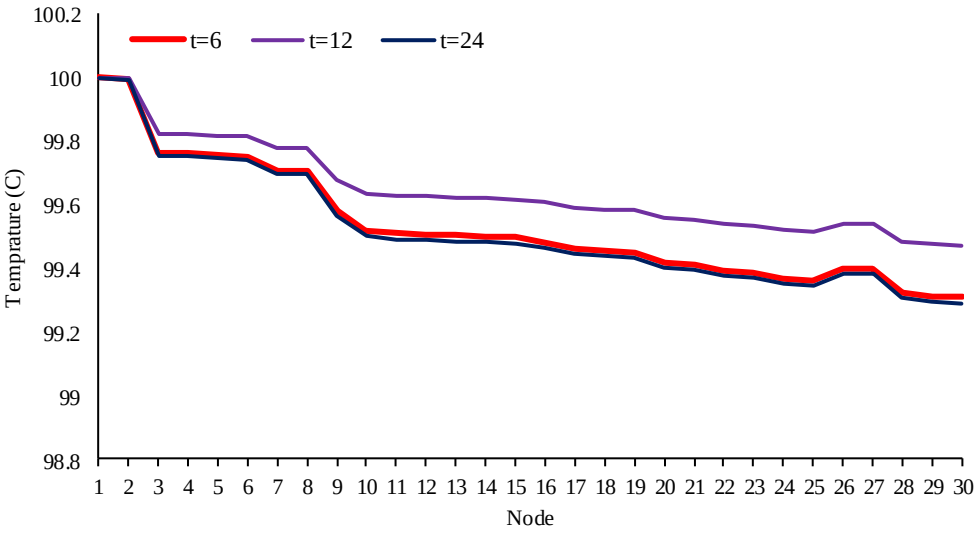

Fig.10. Temperature drops along the pipes

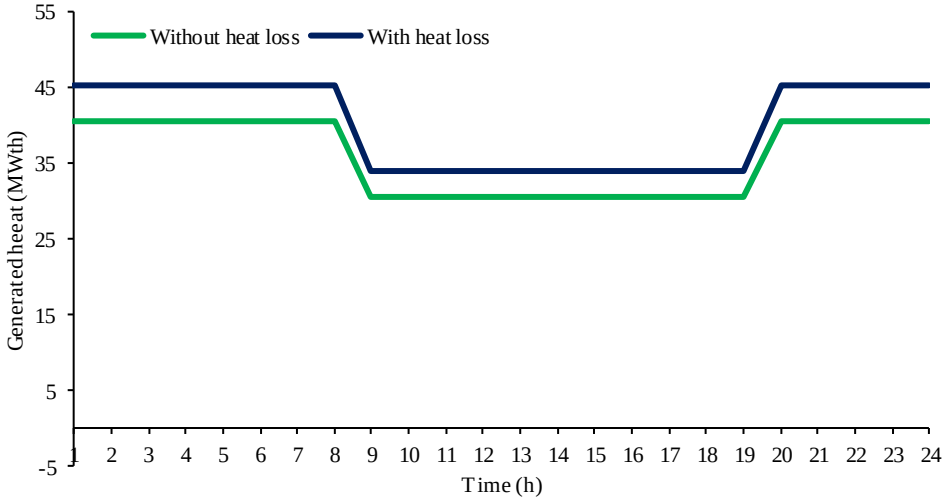

Fig. 11. The effect of heat loss on the generated heat by CHP

Table 4. The impact of consideration of heat loss in coordinated networks

	Without heat loss	With heat loss
Total operation cost ($)	257128.84	259084.19
Electrical operation cost ($)	8867.107	11728.39
Natural gas operation cost (kcf)	248261.74	247355.8
Total generated heat by CHP (MWth)	856.82	960.24
Total generated power by CHP (MW)	4076.19	4054.54

Case 3: In this case, energy storage systems are evaluated as separate and under a coordinated framework.

- **Economic evaluation of thermal storage:** In this case, only the thermal storage system is considered. A thermal storage system is located in the node 1 of the heating system. Figs. 12 and 13 demonstrate hourly scheduling of the thermal storage system and its impact on the hourly dispatch of the CHP plant and the expensive non-gas-fired G1 power plant. As can be seen in these figures, during the hours that the heat storage system is in production mode, it has increased the power dispatch of the CHP plant because the gas fuel is consumed by the CHP power plant to generate power instead of producing heat. Therefore, the hourly participation and dispatch of the power of the expensive G1 plant decrease by increasing the power distribution of the CHP plant. The total cost of operation of the system has been reduced from $259084.19 without a heat storage system to $258363.26 applying a heat storage system.

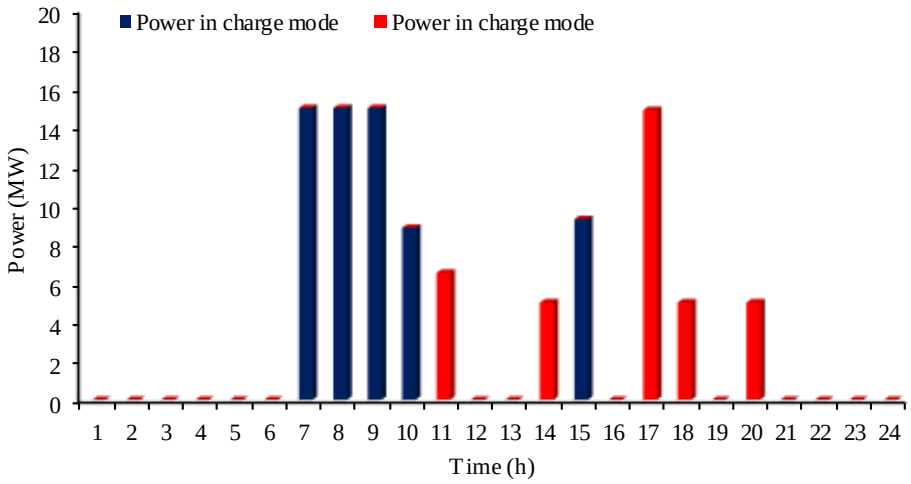

Fig. 12. Charge and discharge power of the heat storage

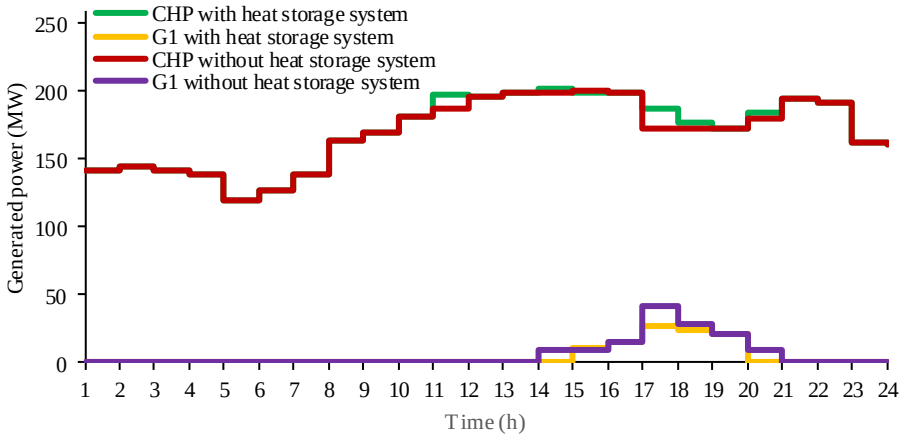

Fig. 13. The effect of the heat storage system on the power generation of plants

- **Economic evaluation of gas storage:** In this case, a gas storage system is located at node 1 of the gas network. Charging, discharging scheduling of natural gas storage, and its effect on the hourly dispatch of power plants are shown in Fig 14 and are reported in Table 5. As it is obvious from this figure, during the hours that the power generation of the CHP plant has been reduced due to its lack of gas supply, the gas storage unit has injected gas into the natural gas system. Therefore, the power production of the CHP plant is increased, which resulted in reducing the participation of expensive power plants and reducing the operation

cost. The operation cost, in this case, is $257686.41, which is lower than the state without storage unit (i.e., $259084.19).

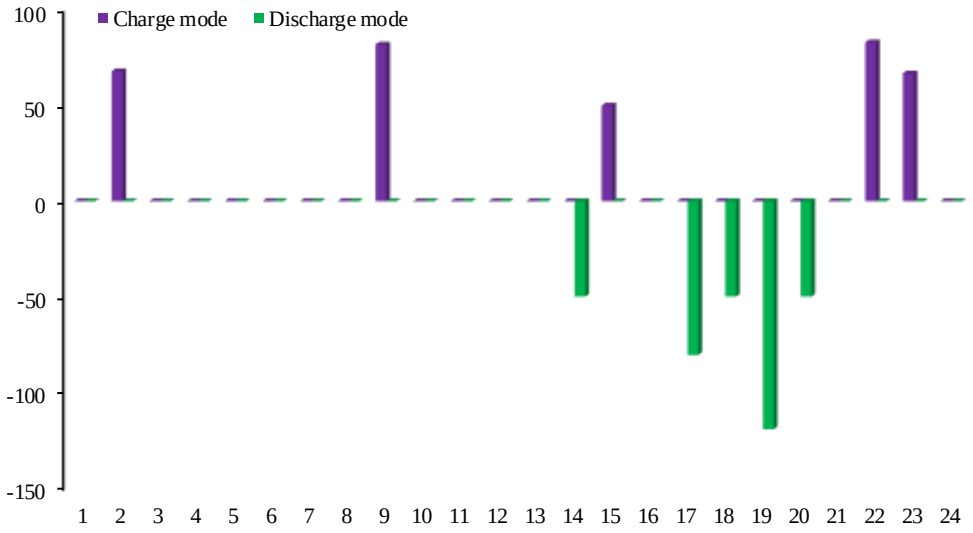

Fig. 14. Charge and discharge of the gas storage

Table 5. The impact of gas storage on hourly dispatch of plants

Time (h)	Without gas storage			With gas storage		
	CHP	G1	G2	CHP	G1	G2
1	142.410	0	0	142.410	0	0
2	144.090	0	0	144.090	0	0
3	141.290	0	0	141.290	0	0
4	138.150	0	0	138.150	0	0
5	119.220	0	0	119.220	0	0
6	126.780	0	0	126.780	0	0
7	138.110	0	0	138.110	0	0
8	163.720	0	0	163.720	0	0
9	169.160	0	0	169.160	0	0
10	181.520	0	0	181.520	0	0
11	186.890	0	10.000	186.890	0	10.000
12	196.820	0	0	196.820	0	0
13	199.479	0	12.841	199.479	0	12.841
14	199.479	10.000	10.601	200.963	0	19.117
15	200.963	10.000	19.417	199.827	10.553	20.000
16	199.479	16.031	20.000	199.479	16.031	20.000
17	172.120	41.720	20.000	186.258	27.582	20.000
18	172.120	29.220	20.000	180.892	20.448	20.000
19	172.120	20.950	20.000	193.070	0	20.000
20	180.074	10.000	10.036	188.846	0	11.264
21	195.150	0	10.000	195.150	0	10.000
22	191.060	0	0	191.060	0	0
23	162.950	0	0	162.950	0	0

24	161.390	0	0	161.390	0	0

- **Economic evaluation of power storage:** In this case, the effect of the power storage system on the optimal operation of multi-carrier energy networks has been investigated. Fig. 15 demonstrates the energy level in the CAES system in the whole scheduling time interval. As it can be seen in this figure, the CAES system is in charge mode between t=7 and t=12. Then, when abundant fuel is not supplied to the CHP plant, the CAES system is in production mode, which results in reducing the contribution of expensive power plants in demand-supply. Table 6 reports the effect of the CAES system on the operation of the integrated electricity, gas and heat systems. As shown in this Table, the CAES system, as an ideal auxiliary option, reduces the operation cost of the electricity system.

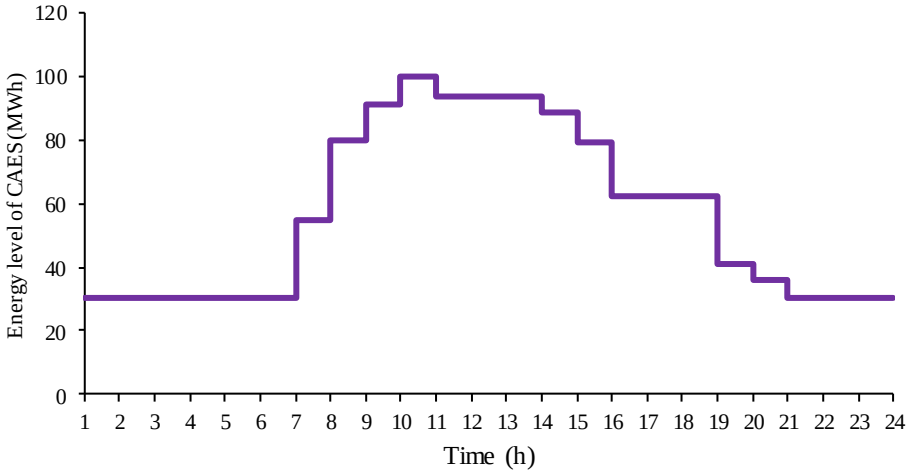

Fig. 15. Energy storage level in CAES

Table 6. The effect of CAES on total operation cost

	Without CAES	With CAES
Total operation cost ($)	259084.19	257475.87
Electrical operation cost ($)	11728.39	5458.82
Natural gas operation cost ($)	247355.80	252017.05

- **Economic evaluation of energy storage systems under a coordinated framework:** In this case, all three energy storage systems are considered simultaneously. Table 7 provides the advantages of simultaneous consideration of these energy storage technologies. Simultaneous consideration of these storage technologies has prevented the contribution of the expensive power plant G1 in all time intervals which leads to a decrease in the power system operation cost. So, simultaneous consideration of energy storage systems has reduced the operation cost of the integrated energy system by 1.3% which can be seen in this Table.

Table 7. The effect of multi-carrier energy storage systems in the total operation cost of integrated energy systems

Storages	-	Thermal	Gas	Power	Thermal+gas+power
Total operation cost ($)	259093.001	258363.26	257686.41	257475.87	255719.54
Electrical operation cost ($)	11728.393	8416.91	6409.348	5458.82	0
Natural gas operation cost ($)	247364.608	249946.35	251277.06	252017.03	255719.54

Case 4: In this case, the effect of multi-carrier energy storage systems on the uncertainty of the wind is investigated. In order to model wind power uncertainty, an IGDT approach has been used to model the uncertainty in wind power production under two risk-averse and risk-seeker strategies without the need for a probability density function. In order to apply the IGDT approach, first, the operation cost in the base condition is calculated, which is $259084.196, in which the multi-carrier energy storage systems are not taken into account in the calculation of this cost. Two risk-averse and risk-seeker strategies are implemented. The parameter E_r is increased from 0.005 to 0.02 with steps of 0.005 in order to apply the IGDT method based on a risk-averse approach, where the network operator considers a robust approach against the uncertainty of wind power. As shown in Fig. 16, the optimal robust function α increases by an increment of the E_r robust parameter, which means that the network operator considers a more robust approach against the uncertainty of the

wind power by an increment of the E_r. Consequently, the network operator considers a higher operation cost for the day-ahead scheduling of the multi-carrier energy systems. For example, the optimal robust function α is 0.094 for E_r=0.005 without the presence of multi-pregnancy storage systems. This means that by 0.5% increase in operation cost, the maximum prediction error in wind power production for the system operator is equal to 0.094, and the hourly distribution of power plants is based on this forecasted error. In Fig. 16, the effect of multi-carrier energy storage systems on wind power uncertainty is shown under the risk-averse strategy. As it is obvious from this figure, the optimal robust function α takes larger values with the presence of multi-carrier energy storage systems, which means that a wider range of prediction errors in wind power production is acceptable under a certain operation cost with the presence of multi-carrier energy storage systems. For example, to reach the specific operation cost of $(1+0.02)*259084.196, the maximum acceptable errors in predicting wind power with and without the presence of multi-carrier energy storage systems are 0.346 and 0.55, respectively. This indicates that multi-carrier energy storage systems can make significant contributions to the risk-averse approach.

In order to apply the risk-seeker based IGDT approach, the opportunity parameter E_ρ is increased from 0.005 to 0.02, which decreases the operation cost compared to its base value. As seen in Fig. 17, the opportunity function β is increased by an increment of the opportunity parameter E_ρ. For example, under E_ρ=0.002, the opportunity function β without the presence of multi-carrier energy storage systems is 0.394, which means that to achieve the desired cost of $(1-0.02) *259084.196, the least acceptable prediction error in the wind power generation is 0.394, and the operator does not attain its desired operation cost when the prediction error is less than 0.394. Also, under the optimal operation cost of $(1-0.02)*259084.196, when multi-carrier energy storage technology is considered, the optimum opportunity function is reduced to 0.152. This means that in the presence

of multi-carrier energy storage technologies, the system operator can achieve its optimal operation at a lower prediction error. For this reason, the multi-carrier energy storage technologies are capable of playing a positive role in the system operation in both risk-seeker and risk-averse strategies.

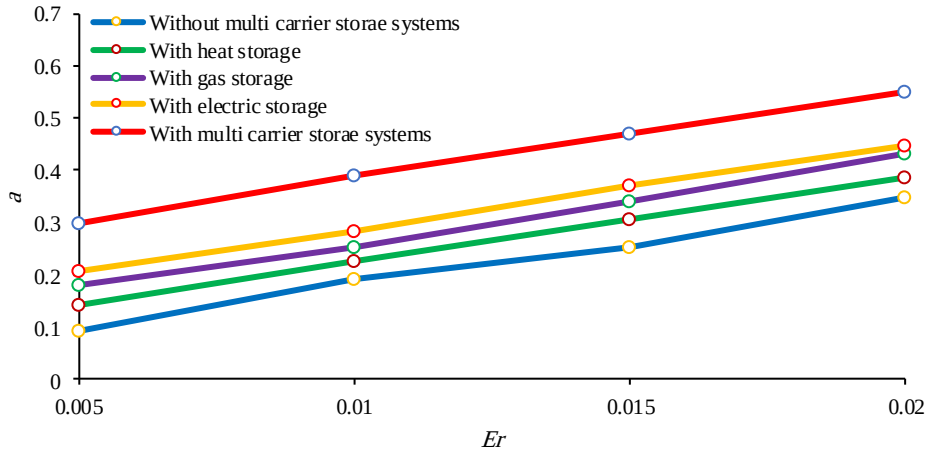

Fig. 16. The effect of the *Er* robust parameter on robust function α

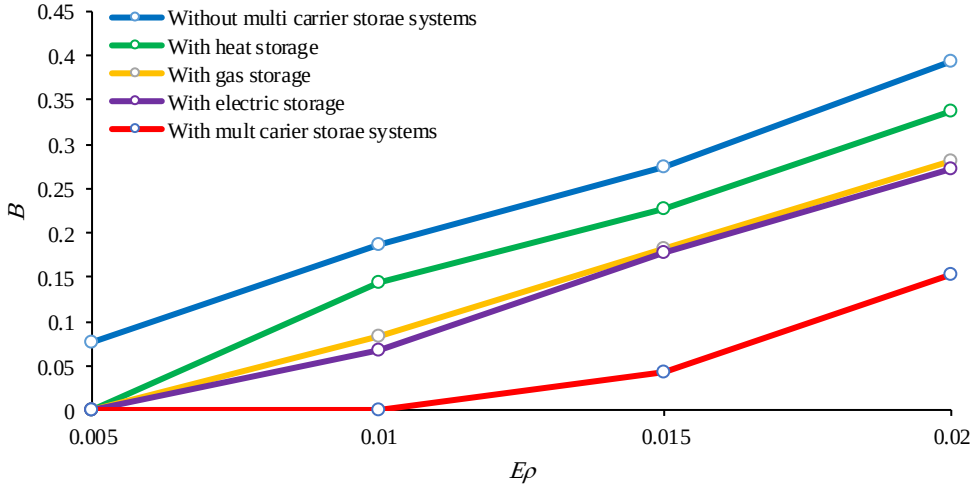

Fig. 17. The effect of $E\rho$ on the opportunity function β

5. Conclusions

This paper proposed the optimal dispatch of an integrated energy system considering wind power uncertainty and related constraints of the natural gas and district heating networks. The information gap-decision theory (IGDT) approach was used for modeling the wind power uncertainty, enabling the operator of the integrated energy system to consider two risk-seeker and risk-averse strategies without the need for a probability density function of the uncertain parameter. Such a method could increase the decision-making range under different strategies. The proposed model was a bi-level problem that was converted to a single-level problem with a simple concept without the need to apply the Karush–Kuhn–Tucker (KKT) conditions. In addition, the effect of multi-carrier energy storage systems was examined on the operation of integrated systems. Simulation results demonstrated that:

- The operation cost of the power system increased by 11% due to a drop in gas pressure when the residential gas load increased. Also, the generated heat by the combined heat and power (CHP) unit increased by 10% when heat loss of DHN was considered.
- Multi-carrier energy storage systems reduced the operation cost of the integrated system by 1.3%.
- Multi-carrier energy storage systems could reduce the effect of the uncertainty of wind power production on the operation cost of the entire system by 20%.
- Multi-carrier energy storage technologies could have a two-fold advantage: in the risk-averse strategy, it helps the network operator to implement the strategy with a higher reliability level by 20%, while in a risk-seeker approach, such technologies help the network operator to implement their own risk-seeker strategy under lower risk levels by 60%.

Reference

[1] M. Hemmati, B. Mohammadi-Ivatloo, S. Ghasemzadeh, and E. Reihani, "Risk-based optimal scheduling of reconfigurable smart renewable energy based microgrids," *International Journal of Electrical Power & Energy Systems*, vol. 101, pp. 415-428, 2018.

[2] M. Hemmati, S. Ghasemzadeh, and B. Mohammadi-Ivatloo, "Optimal scheduling of smart reconfigurable neighbour micro-grids," *IET Generation, Transmission & Distribution*, vol. 13, pp. 380-389, 2018.

[3] M. Nazari-Heris, S. Abapour, and B. Mohammadi-Ivatloo, "Optimal economic dispatch of FC-CHP based heat and power micro-grids," *Applied Thermal Engineering*, vol. 114, pp. 756-769, 2017.

[4] T. H. Kwan, X. Wu, and Q. Yao, "Performance comparison of several heat pump technologies for fuel cell micro-CHP integration using a multi-objective optimisation approach," *Applied Thermal Engineering*, vol. 160, p. 114002, 2019.

[5] M. Majidi, B. Mohammadi-Ivatloo, and A. Anvari-Moghaddam, "Optimal robust operation of combined heat and power systems with demand response programs," *Applied Thermal Engineering*, vol. 149, pp. 1359-1369, 2019.

[6] A. Alabdulwahab, A. Abusorrah, X. Zhang, and M. J. I. T. o. S. E. Shahidehpour, "Coordination of interdependent natural gas and electricity infrastructures for firming the variability of wind energy in stochastic day-ahead scheduling," vol. 6, pp. 606-615, 2015.

[7] H. Wang, L. Duanmu, R. Lahdelma, and X. Li, "A fuzzy-grey multicriteria decision making model for district heating system," *Applied Thermal Engineering*, vol. 128, pp. 1051-1061, 2018.

[8] G. Comodi, M. Lorenzetti, D. Salvi, and A. Arteconi, "Criticalities of district heating in Southern Europe: Lesson learned from a CHP-DH in Central Italy," *Applied Thermal Engineering*, vol. 112, pp. 649-659, 2017.

[9] M. Nazari-Heris, B. Mohammadi-Ivatloo, G. B. Gharehpetian, and M. J. I. S. J. Shahidehpour, "Robust short-term scheduling of integrated heat and power microgrids," pp. 1-9, 2018.

[10] B. C. Erdener, K. A. Pambour, R. B. Lavin, and B. Dengiz, "An integrated simulation model for analysing electricity and gas systems," *International Journal of Electrical Power & Energy Systems*, vol. 61, pp. 410-420, 2014.

[11] L. Bai, F. Li, H. Cui, T. Jiang, H. Sun, and J. Zhu, "Interval optimization based operating strategy for gas-electricity integrated energy systems considering demand response and wind uncertainty," *Applied Energy*, vol. 167, pp. 270-279, 2016.

[12] Q. Zeng, J. Fang, J. Li, and Z. Chen, "Steady-state analysis of the integrated natural gas and electric power system with bi-directional energy conversion," *Applied energy*, vol. 184, pp. 1483-1492, 2016.

[13] Y. Zhang, Y. Hu, J. Ma, and Z. Bie, "A Mixed-integer Linear Programming Approach to Security-constrained Co-optimization Expansion Planning of Natural Gas and Electricity Transmission Systems," *IEEE Transactions on Power Systems*, 2018.

[14] H. Cui, F. Li, Q. Hu, L. Bai, and X. Fang, "Day-ahead coordinated operation of utility-scale electricity and natural gas networks considering demand response based virtual power plants," *Applied Energy*, vol. 176, pp. 183-195, 2016.

[15] G. Li, R. Zhang, T. Jiang, H. Chen, L. Bai, and X. Li, "Security-constrained bi-level economic dispatch model for integrated natural gas and electricity systems considering wind power and power-to-gas process," *Applied energy*, vol. 194, pp. 696-704, 2017.

[16] M. Nazari-Heris, M. A. Mirzaei, B. Mohammadi-Ivatloo, M. Marzband, and S. Asadi, "Economic-environmental effect of power to gas technology in coupled electricity and gas systems with price-responsive shiftable loads," *Journal of Cleaner Production*, p. 118769, 2019.

[17] Q. Zeng, B. Zhang, J. Fang, and Z. Chen, "A bi-level programming for multistage co-expansion planning of the integrated gas and electricity system," *Applied energy*, vol. 200, pp. 192-203, 2017.

[18] X. Zhang, M. Shahidehpour, A. Alabdulwahab, and A. Abusorrah, "Hourly electricity demand response in the stochastic day-ahead scheduling of coordinated electricity and natural gas networks," *IEEE Transactions on Power Systems,* vol. 31, pp. 592-601, 2016.
[19] C. Shao, X. Wang, M. Shahidehpour, X. Wang, and B. Wang, "An MILP-based optimal power flow in multicarrier energy systems," *IEEE Trans. Sustain. Energy,* vol. 8, pp. 239-248, 2017.
[20] M. A. Mirzaei, A. S. Yazdankhah, B. Mohammadi-Ivatloo, M. Marzband, M. Shafie-khah, and J. P. Catalão, "Stochastic network-constrained co-optimization of energy and reserve products in renewable energy integrated power and gas networks with energy storage systems," *Journal of Cleaner Production,* 2019.
[21] M. A. Mirzaei, A. Sadeghi-Yazdankhah, B. Mohammadi-Ivatloo, M. Marzband, M. Shafie-khah, and J. P. Catalão, "Integration of emerging resources in IGDT-based robust scheduling of combined power and natural gas systems considering flexible ramping products," *Energy,* vol. 189, p. 116195, 2019.
[22] Y. He, M. Shahidehpour, Z. Li, C. Guo, and B. Zhu, "Robust constrained operation of integrated electricity-natural gas system considering distributed natural gas storage," *IEEE Transactions on Sustainable Energy,* vol. 9, pp. 1061-1071, 2017.
[23] C. He, L. Wu, T. Liu, W. Wei, and C. Wang, "Co-optimization scheduling of interdependent power and gas systems with electricity and gas uncertainties," *Energy,* vol. 159, pp. 1003-1015, 2018.
[24] C. Lin, W. Wu, B. Wang, M. Shahidehpour, and B. Zhang, "Joint Commitment of Generation Units and Heat Exchange Stations for Combined Heat and Power Systems," *IEEE Transactions on Sustainable Energy,* 2019.
[25] Z. Li, W. Wu, J. Wang, B. Zhang, and T. Zheng, "Transmission-constrained unit commitment considering combined electricity and district heating networks," *IEEE Transactions on Sustainable Energy,* vol. 7, pp. 480-492, 2016.
[26] A. Najafi, H. Falaghi, J. Contreras, and M. J. A. E. Ramezani, "Medium-term energy hub management subject to electricity price and wind uncertainty," vol. 168, pp. 418-433, 2016.
[27] Y. ali Shaabani, A. R. Seifi, and M. J. J. E. Kouhanjani, "Stochastic multi-objective optimization of combined heat and power economic/emission dispatch," vol. 141, pp. 1892-1904, 2017.
[28] G. Li, R. Zhang, T. Jiang, H. Chen, L. Bai, and X. J. A. e. Li, "Security-constrained bi-level economic dispatch model for integrated natural gas and electricity systems considering wind power and power-to-gas process," vol. 194, pp. 696-704, 2017.
[29] M. Alipour, B. Mohammadi-Ivatloo, and K. J. I. T. o. I. I. Zare, "Stochastic scheduling of renewable and CHP-based microgrids," vol. 11, pp. 1049-1058, 2015.
[30] M. Alipour, K. Zare, and H. J. E. Seyedi, "A multi-follower bilevel stochastic programming approach for energy management of combined heat and power micro-grids," vol. 149, pp. 135-146, 2018.
[31] J. Li, J. Fang, Q. Zeng, and Z. Chen, "Optimal operation of the integrated electrical and heating systems to accommodate the intermittent renewable sources," *Applied Energy,* vol. 167, pp. 244-254, 2016.
[32] S. Lu, W. Gu, J. Zhou, X. Zhang, and C. Wu, "Coordinated dispatch of multi-energy system with district heating network: Modeling and solution strategy," *Energy,* vol. 152, pp. 358-370, 2018.
[33] A. Shabanpour-Haghighi and A. R. Seifi, "Effects of district heating networks on optimal energy flow of multi-carrier systems," *Renewable and Sustainable Energy Reviews,* vol. 59, pp. 379-387, 2016.
[34] A. Shabanpour-Haghighi and A. R. Seifi, "Simultaneous integrated optimal energy flow of electricity, gas, and heat," *Energy conversion and management,* vol. 101, pp. 579-591, 2015.
[35] A. Shabanpour-Haghighi and A. R. Seifi, "Multi-objective operation management of a multi-carrier energy system," *Energy,* vol. 88, pp. 430-442, 2015.
[36] Y. Li, Y. Zou, Y. Tan, Y. Cao, X. Liu, M. Shahidehpour, *et al.*, "Optimal stochastic operation of integrated low-carbon electric power, natural gas, and heat delivery system," *IEEE Transactions on Sustainable Energy,* vol. 9, pp. 273-283, 2018.

[37] E. A. M. Ceseña and P. Mancarella, "Energy Systems Integration in Smart Districts: Robust Optimisation of Multi-Energy Flows in Integrated Electricity, Heat and Gas Networks," *IEEE Transactions on Smart Grid,* vol. 10, pp. 1122-1131, 2019.
[38] M. A. Mirzaei, M. Nazari-Heris, B. Mohammadi-Ivatloo, K. Zare, M. Marzband, and A. Anvari-Moghaddam, "A Novel Hybrid Framework for Co-Optimization of Power and Natural Gas Networks Integrated With Emerging Technologies," *IEEE Systems Journal,* 2020.
[39] A. O'Connell, A. Soroudi, and A. Keane, "Distribution network operation under uncertainty using information gap decision theory," *IEEE Transactions on Smart Grid,* vol. 9, pp. 1848-1858, 2018.
[40] N. Rezaei, A. Ahmadi, A. H. Khazali, and J. M. Guerrero, "Energy and frequency hierarchical management system using information gap decision theory for islanded microgrids," *IEEE Transactions on Industrial Electronics,* vol. 65, pp. 7921-7932, 2018.
[41] A. Najafi-Ghalelou, S. Nojavan, and K. Zare, "Heating and power hub models for robust performance of smart building using information gap decision theory," *International Journal of Electrical Power & Energy Systems,* vol. 98, pp. 23-35, 2018.
[42] A. Soroudi, A. Rabiee, and A. Keane, "Information gap decision theory approach to deal with wind power uncertainty in unit commitment," *Electric Power Systems Research,* vol. 145, pp. 137-148, 2017.
[43] A. Nikoobakht and J. Aghaei, "IGDT-based robust optimal utilisation of wind power generation using coordinated flexibility resources," *IET Renewable Power Generation,* vol. 11, pp. 264-277, 2016.
[44] A. Alabdulwahab, A. Abusorrah, X. Zhang, and M. Shahidehpour, "Stochastic security-constrained scheduling of coordinated electricity and natural gas infrastructures," *IEEE Systems Journal,* 2015.

Appendix

Table A1. Fuel coefficients of the CHP unit

Unit	*a* (kcf/MW^{2}h)	*b* (kcf/MWh)	*c* (kcf/h)	*d* *(kcf/MWth)*	*e* *(kcf/MWth)*	f ($/MWth)
CHP	0.0172	7.2	55.205	0.015	2.1	0.031

Table A2. Characteristics of CHP unit

P^A , P^B, P^C, P^D *(MW)*	H^A ,H^B,H^C, H^D (MWth)	Initial Status (h)	Min Down (h)	Min Up (h)	Ramp (MW/h)
205, 178, 66, 80	0, 150, 85, 0	1	1	1	55

Table A3. fuel coefficients and characteristics of plant G2

Unit	*a* (kcf/MW^{2}h)	*b* (kcf/MWh)	*c* (kcf/h)	P_{max} (MW)	P_{min} (MW)	Initial Status (h)	Min Down (h)	Min Up (h)	Ramp (MW/h)
G2	0.0025	8.85	68.705	20	10	-1	1	1	20

Table A4. Cost coefficients and characteristics of plant G1

Unit	a ($/MW^{2}h)	b ($MWh)	c ($/h)	P_{max} (MW)	P_{min} (MW)	Initial Status (h)	Min Down (h)	Min Up (h)	Ramp (MW/h)
G1	0.001	32.63	129.97	100	10	-3	3	2	50

Table A5. Thermal storage system parameters

B_{hs}^{Max} (MWh)	B_{hs}^{Min} (MWh)	$B_{hs}^{\text{Max, charge}}$ (MWh)	$B_{hs}^{\text{Max, discharge}}$ (MWh)	$B_{hs}^{\text{Min, charge}}$ (MWh)	$B_{hs}^{\text{Min, discharge}}$ (MWh)	η_{hs}^{ch} , η_{hs}^{dis}	η_{hs}
60	0	15	15	0	0	0.9	0.95

Table A6. CAES system parameters

$A_e^{\max}$ (MWh)	$A_e^{\min}$ (MWh)	$P_e^{D,\text{Max}}$ (MW)	$P_e^{D,\text{Min}}$ (MW)	$P_e^{C,\text{Max}}$ (MW)	$P_e^{C,\text{Min}}$ (MW)	η_e^C , η_e^D	HR_e (kcf/MWh)
100	30	25	5	25	5	0.9	4.102

Table A7. Gas storage system parameters

$E_{gs}^{\max}$ (kcf)	$E_{gs}^{\min}$ (kcf)	$GS_{gs,\max}^{out}$ (kcf)	$GS_{gs,\max}^{in}$ (kcf)
300	0	100	100